PCCP

PAPER

View Article Online
View Journal | View Issue

Cite this: *Phys. Chem. Chem. Phys.*, 2014, **16**, 5213

DFT study on the atomic-scale nucleation path of graphene growth on the Cu(111) surface†

Yingfeng Li,[a] Meicheng Li,*[ab] Tai Wang,[a] Fan Bai[c] and Yang-Xin Yu*[d]

Received 10th October 2013,
Accepted 17th January 2014

DOI: 10.1039/c3cp54275k

www.rsc.org/pccp

The nucleation path of graphene growth on the Cu(111) surface is investigated by importing carbon atoms step-by-step using density functional theory (DFT) calculations. An overall path of graphene nucleation has been proposed based on configuration and energy analysis. At the very first stage, linear chains will be formed and dominate the copper surface. Then, Y-type (furcate) carbon species will be shaped when new carbon atoms are absorbed aside the linear chains. Finally, ring-containing carbon species and graphene islands will be formed stepwise, with energetic preference. We find that the Y-type and ring-containing carbon species are not likely formed directly at the initial stage of graphene nucleation, but should be formed starting from linear chains. The nucleation limiting step is the formation of the Y-type species, which must pass an energy barrier of about 0.25 eV. These underlying observations are instructive to stimulate future experimental efforts on graphene synthesis.

1. Introduction

To fully exploit the potential application[1–3] of graphene, reliable production of high-quality samples in large quantity is a prerequisite. Recently, large area, high-quality graphene has been synthesized on a copper substrate by the chemical vapor deposition (CVD) method.[4–6] But such obtained graphene samples still display considerable imperfections such as wrinkles and grain boundaries. Based on characterization using transmission electron microscopy, Rasool *et al.*[7] suggested that the quality of graphene is ultimately limited by nucleation at the surface of the copper catalyst. So, to further improve the synthesis technology of graphene, a deep understanding of the fundamentals of its nucleation process on the copper surface is required.

By experimental methods, the growth mechanism of graphene on the copper substrate has been demonstrated to be a surface adsorption process,[8,9] and some mesoscopic structure evolution[10,11] and other[12] details during its growth have been revealed. But with experimental technologies, nowadays, it is still very difficult to probe into graphene nucleation at the atomic scale. Atomistic simulation methods, like Monte Carlo and molecular dynamics, can be used to reveal the self-organization of carbon atoms on a metal surface,[13–16] but their precision and reliability depend dramatically on the potential functions being used. The first principles method, starting directly at the level of established science, does not make assumptions such as an empirical model and fitting parameters, and can provide more precise and reliable results than atomistic simulations methods. With the aid of the first principles method, some efforts focusing on the atomic-scale details of graphene nucleation on copper[17–25] and other metals[26–28] have been made. For example, it has been found that two carbon atoms prefer to form a dimer on the Cu(111) surface.[21,23,29] Partial sinking of carbon atoms into the Cu(111) subsurface was first suggested in ref. 22, while at low-concentrations, and using large enough unit cells, complete sinking in subsurface octahedral sites should take place.[23] In fact, such sinking and the associated migration barriers are sensitive to copper-lattice mediated stresses and to the size of the computational unit cell.[23] Such lattice-mediated stresses can also result in the complete "up-floating" of carbon atoms at high concentrations and/or when smaller unit cells are being used.[23,24] These results confirm the growth mechanism discovered by experiments,[9] and indicate that an on-surface coalescence process of carbon atoms step-by-step should dominate the nucleation of graphene on the copper surface. Van Wesep *et al.*[25] have shown that linear chains would dominate on the surface when cluster sizes are less than about ten adatoms, by comparing the formation energies of one-dimensional linear chains and two-dimensional compact islands

[a] *State Key Laboratory of Alternate Electrical Power System with Renewable Energy Sources, North China Electric Power University, Beijing, 102206, PR China. E-mail: mcli@ncepu.edu.cn*
[b] *Suzhou Institute, North China Electric Power University, Suzhou, 215123, PR China*
[c] *School of Materials Science and Engineering, Harbin Institute of Technology, Harbin, 150001, PR China*
[d] *Laboratory of Chemical Engineering Thermodynamics, Department of Chemical Engineering, Tsinghua University, Beijing, 100084, PR China. E-mail: yangxyu@mail.tsinghua.edu.cn*

† Electronic supplementary information (ESI) available. See DOI: 10.1039/c3cp54275k

of equal sizes on the Cu(111) surface. In their work, only one kind of but no other possible two-dimensional compact configurations (like branched chains) has been taken into account. As far as we know, there is still no report on the fundamental question that how a graphene island is nucleated on the copper surface starting from an isolated carbon atom by coalescing more carbon atoms step-by-step, and taking all kinds of possible structural motifs into account for each step.

The aim of this work is to provide a clear atomic picture for the step-by-step nucleation process of graphene growth on the Cu(111) surface. Using density functional theory (DFT) calculations, the overall nucleation path of graphene growth on the copper surface is systematically studied by importing carbon atoms stepwise. This work represents an important step in revealing the whole growth process of graphene, and is helpful to guide the experimental synthesis of it.

2. Calculation details

All calculations were conducted using the DFT integrated in the Dmol^3 model[30,31] in Materials Studio of Accelrys Inc. The double-ζ numerical basis set with polarization functions (DNP) and DFT semicore pseudopotential (DSPP) were used, and the electron exchange and correlation effects were described by the Perdew–Burker–Ernzerhof (PBE) method,[32] a generalized gradient approximation (GGA)-type exchange–correlation function. During our calculations, the real-space cutoff of a plane wave was set at 4.4 Å; the *k*-point mesh was set to 2 × 2 × 1; and no Fermi smearing was adopted. The cutoff value and *k*-point sampling were carefully tested to produce converged results. The tolerances of energy, gradient, and displacement convergence were set as 1×10^{-5} hartree, 2×10^{-3} hartree Å^{-1} and 5×10^{-3} Å, respectively. And the self-consistent-field (SCF) density convergence threshold value was set at 1×10^{-6} hartree.

The Cu(111) facet was simulated using a periodic 4-layer slab of 4 × 4 supercells, which contains 64 copper atoms. Repeated slabs are separated by about 10 Å vacuum to avoid interactions between neighboring slabs, and the final lattice parameters used are 10.224 Å × 10.224 Å × 19.0608 Å. During our calculations, the bottom two layers of copper atoms were fixed, whereas the top two layers were allowed to relax.

Carbon atoms were imported stepwise on the Cu(111) surface. Once a new carbon atom was imported, the geometry of the system was reoptimized with aforementioned sets. The adsorption energies E_{ads} per carbon atom are defined as

$$E_{ads} = \frac{E_{nc+surface} - E_{surface} - n\mu}{n} \quad (1)$$

where $E_{nc+surface}$ stands for the energy of a system having carbon species adsorbed on the copper surface, $E_{surface}$ is the energy of a clear copper surface, and μ is the energy of an isolated carbon atom under vacuum. Quantity n denotes the number of carbon atoms in the carbon species. With this definition, negative adsorption energies would be obtained, which correspond to exothermic adsorption.

3. Results and discussion

3.1 The nucleation process from an isolated carbon to a 3-membered chain

At first, the nucleation process of graphene from an isolated carbon atom to a 3-membered carbon species (labeled C1 to C3 in Fig. 1, respectively) on the Cu(111) surface is studied by importing carbon atoms step-by-step. The stable on-surface configurations obtained and the corresponding adsorption energies per carbon atom are given in Fig. 1.

Since there are two inequivalent sites (HCP and FCC, illustrated in Conf. C1) for carbon adsorption on the Cu(111) surface, both carbon species C1 and C3 appear in two stable configurations. Configuration C3-a consists of two carbon atoms sitting in the HCP with one atom sitting in the FCC site, while C3-b consists of two carbon atoms sitting in the FCC with one atom sitting in the HCP site. The on-surface carbon species being formed in this nucleation stage only have one type of topology, *i.e.* linear type. The results obtained in this section provide the foundation for the following investigations.

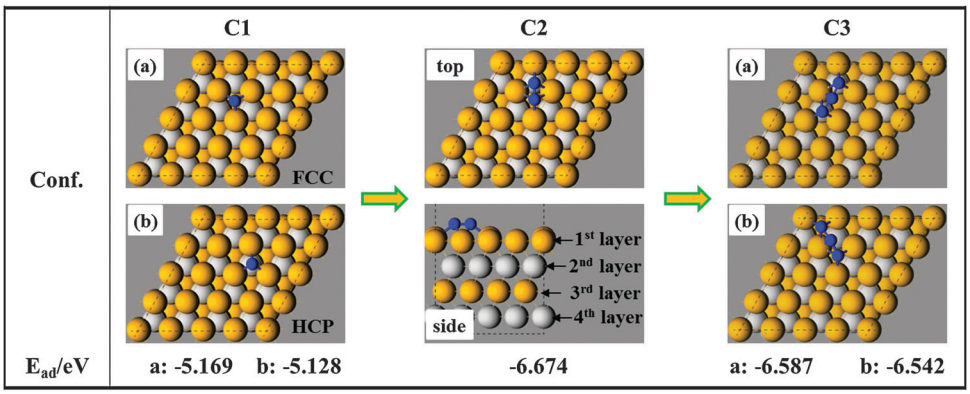

Fig. 1 The stable configurations and adsorption energies from an isolated carbon atom to a 3-membered carbon species on the Cu(111) surface. Only the top views of C1 and C3, and both the top and side views of C2 are given. Carbon atoms are colored blue. Copper atoms in the 1st and 3rd layers are colored apricot, while that in the 2nd and 4th layers are colored white.

3.2 Evolution tendencies in the nucleation process starting from Conf. C3

Starting from the linear carbon species C3 obtained onward, there should exist three different evolution tendencies in the following nucleation process of graphene: to form linear, Y-type (furcate) and circular topologies of carbon species. These three evolution tendencies are investigated, respectively, below.

3.2.1 Configuration and adsorption energy results of the linear carbon species. Based on the carbon species C3-a presented in Fig. 1, 1 to 3 extra carbon atoms have been placed step-by-step at its tail. After sufficient structural relaxations, four stable configurations are obtained and given in Fig. 2, in which the corresponding adsorption energies per carbon atom are also provided. Using the same reason mentioned in Section 3.1, the 5-membered linear chains present two stable configurations L5-a, whose tail carbon atoms sitting in two FCC sites, and L5-b, whose tail carbon atoms sitting in the two HCP sites.

Since the adsorption energy per carbon atom only decreases by about 0.1 eV from L4 to L6, we construct a 10-membered linear chain to evaluate this decreasing extent further. The optimized configuration (labeled L10) obtained is given in the ESI,† and the adsorption energy per carbon atom in it is −7.013 eV.

3.2.2 Configuration and adsorption energy results of the Y-type carbon species. Starting from the configurations C3-a and C3-b in Fig. 1, two series of Y-type carbon species, whose central carbon atom is in the FCC and HCP site, respectively, have been obtained. But as these two series of Y-type carbon species represent one and the same nucleation tendency of graphene, only the results of the series having a FCC central carbon atom are given here, whereas that of the other series is supplied in the ESI.†

In Fig. 3, the scheme designed for importing additional carbon atoms and the adsorption sites used is first illustrated, and then the obtained configurations and corresponding adsorption energies per carbon atom are given. The stable Y-type configuration Y4 either has three carbon atoms in the FCC sites and one in the HCP site or three carbon atoms in the HCP sites and one in the FCC site, which is quite different from that on the nickel(111) surface having three carbon atoms in the FCC sites and one in the TOP site.[33]

3.2.3 Configuration and adsorption energy results of the circular carbon species. To simulate a cyclization nucleation process based on the configuration C3-b (or C3-a, which shows similar results and is given in the ESI†), firstly, we import one carbon atom in site1 as shown in Fig. 4. While after structural relaxations, no cyclization tendency is observed but a linear carbon chain (labeled R4) is obtained. So in the next steps, two carbon atoms are imported in site1 and site2 concurrently to increase the probability of forming a circular carbon species. Still no circular but a semi-circular carbon species (labeled R5) is obtained. Finally, another carbon atom is imported in site3, and a much awaited 6-membered carbon ring (labeled R6) is obtained. The scheme, used adsorption sites, final stable configurations and adsorption energies are given in Fig. 4.

Since the linear carbon chain R4 obtained here covers a copper atom and so appears quite different from that of L4 in Fig. 2, some further efforts have been made by adding extra carbon atoms at the two ends of this carbon chain. But as no new phenomenon has been revealed, these results are supplied in the ESI.†

3.2.4 Configuration and adsorption energy analyses. From the configuration results obtained above, the most remarkable observation is the strong preference for the formation of linear carbon species. In the linear nucleation attempts (as shown in Fig. 2), the final configurations keep their linear topologies as designed; in the circular nucleation attempts (Fig. 4), a linear carbon chain R4 is formed through significant configuration adjustments; and in the Y-type nucleation attempts (Fig. 3), despite the topologies being maintained ultimately, each branch in its final configuration shows strong tendency to straighten. So, we deduce that linear chains should be the dominant carbon species at the very first stages of graphene nucleation on the copper surface.

This deduction can be confirmed by the more reliable adsorption energy results. In Fig. 5 we plot the adsorption energies per carbon atom in all of the final configurations obtained above. Obviously, the linear carbon chains show remarkable energetic preference compared to the Y-type and circular carbon species: with equal sizes, the adsorption energy per carbon atom in a linear chain is about 0.3 eV lower than that in a circular

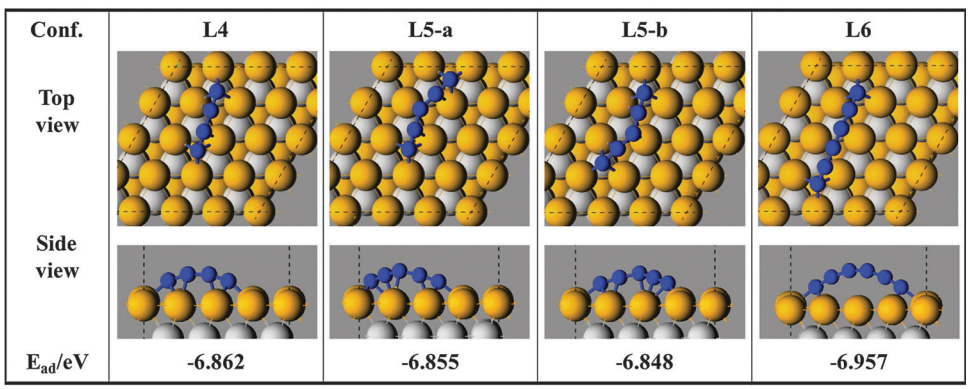

Fig. 2 The stable configurations and corresponding adsorption energies per carbon atom of the linear carbon chains. Both the top and side views are given. The copper and carbon atoms are colored the same as that in Fig. 1.

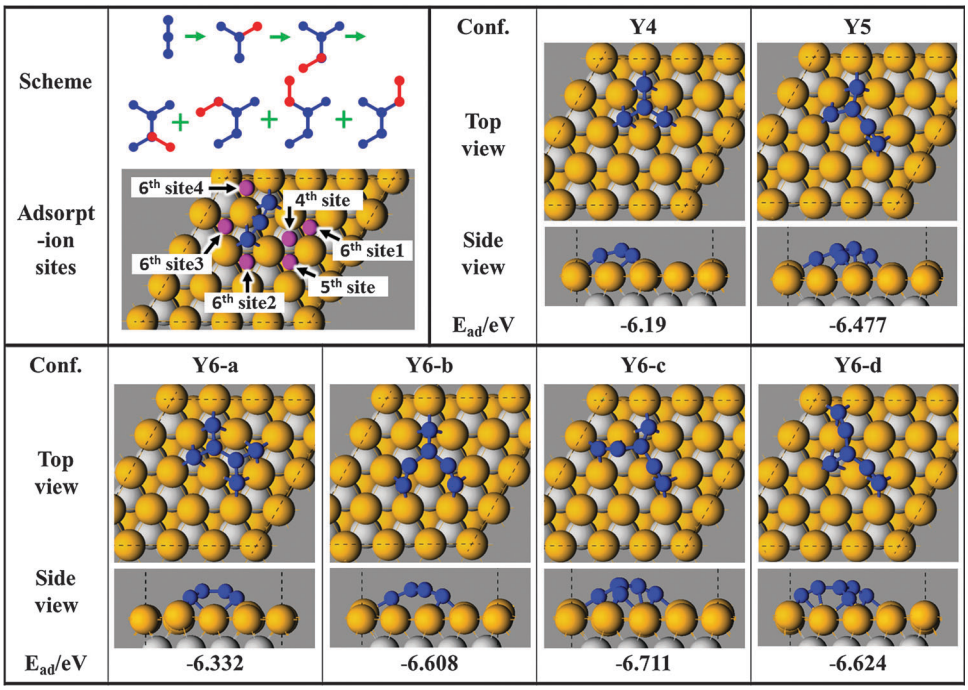

Fig. 3 The scheme designed for importing additional carbon atoms, the adsorption sites used, the stable configurations and corresponding adsorption energies of the Y-type carbon species. Firstly, one carbon atom is imported in the 4th site, then the next carbon atom is imported in the 5th site, and finally another carbon atom is imported in one of the 6th sites.

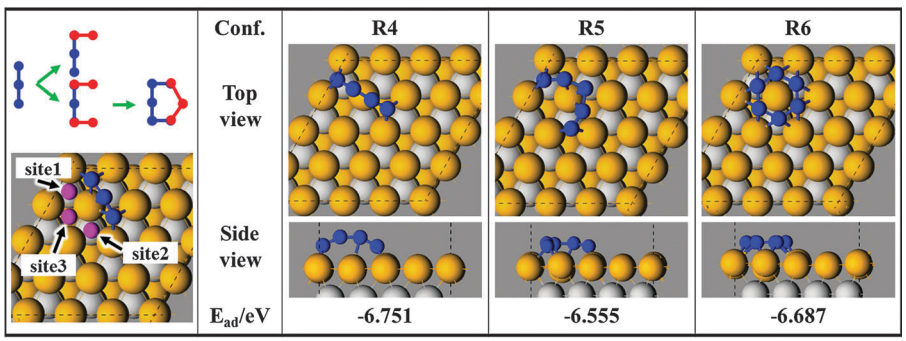

Fig. 4 The scheme, adsorption sites, final stable configurations and adsorption energies of the circular carbon species.

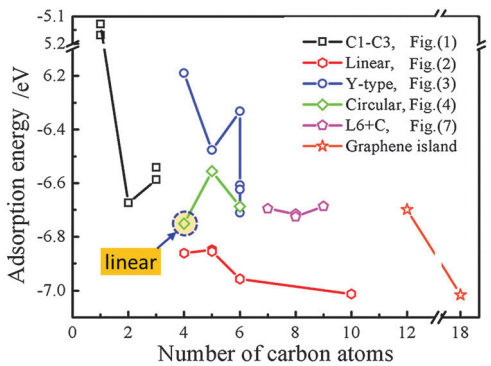

Fig. 5 The adsorption energies per carbon atom *vs.* the number of carbon atoms. The point enclosed by a blue dashed circle corresponds to a linear chain, which covers a copper atom.

carbon species, and even more lower than that in a Y-type carbon species.

The driving force and the energetic preference for the linear growth are analyzed based on comparing the bond lengths of C–C bonds and the shapes of the deformation electrodensities of the linear carbon species on the copper surface with those of standard sp, sp^2 and sp^3 C–C bonds. Being limited by space, the analyses are given in the ESI.† In conclusion, it is the energetic preference for C–C bonds composed of sp hybridized carbon atoms that drives the initial linear growth. The energy dislike for the formation of Y-type and circular carbon species may be able to be attributed to the sp^2 carbon atoms and the bended carbon structure in them, respectively. By taking the configurations and adsorption energies into account together, it could be found that the adsorption energy per carbon atom in Y-type carbon species relates dramatically to the ratio of

sp^2 carbon atoms: that in configurations Y4 and Y6-a (having 1/4 and 1/3 of sp^2 carbon atoms, respectively) displays the biggest value, in Y5 (1/5 sp^2) displays a relatively smaller value, and in Y6-b, c, d (1/6 sp^2) displays the smallest value. The adsorption energy per carbon atom in configuration R5, which shows no intrinsic differences from configuration L5 except for having a sharp bend structure, displays about 0.3 eV higher than that in configuration L5.

Synthesizing the above configuration and energy analyses, it could be concluded that the formation of linear chains should dominate the nucleation process of graphene growth on the copper surface when the cluster sizes are quite small. While, the formation of both Y-type and circular carbon species is quite difficult due to the fact that the formation of sp^2 carbon atoms and bended carbon structure is energetically unfavored. This conclusion is consistent with that in ref. 25 according to the fact that a hexatomic ring is easily broken. This result also manifests that the growth mechanism on the copper surface should be quite different from that on the nickel surface, where a circular species having eight carbon atoms is about 1.7 eV energetically favored than a linear species having the same number of carbon atoms.[34]

After the favored carbon species at the very initial stages of graphene nucleation has been determined, the next important question is to determine the common size of the linear chains on copper surface. As shown clearly in Fig. 5, with the growth of a linear carbon chain, the adsorption energy per carbon atom becomes smaller and smaller. This indicates that formation of longer linear chains is energetically favored. On one side, this energetic preference for a longer linear chain is not very large to support its everlasting growth: the adsorption energy per carbon atom in configuration L10 is merely about 0.15 eV lower than in L4; on the other side, from the aspect of entropy, the formation of long linear carbon chains should also be a small probability event. So, comprehensively, linear chains containing 4 to 10 carbon atoms may dominate the copper surface at the very initial nucleation stages of graphene nucleation.

Further, the bonding situation between the linear chain and the copper surface suggests that a 6-membered linear chain should be a representative carbon species. Fig. 6 shows the deformation electrodensity maps with isovalue 0.01 electrons $Å^{-3}$ for configurations from L4 to L10, in which the green color indicates that net electrons remain and stable chemical bonds are formed. Clearly, when the size of the linear chains is smaller than 6, not only the end- but also the mid-carbon atoms in them have formed stable C–Cu bonds with the copper surface; if the size increases to 6, an arc-shaped carbon chain, whose mid-carbon atoms are completely detached from the copper surface, has formed; and when the size increases continually to 10, the linear chain (L10 in Fig. 6) expresses no new characteristics compared with that of L6 but supports a bigger arch. So, L6 is exactly the transition configuration from an on-surface to an arc-shaped linear carbon chain on the copper surface, and should be a representative structure at the initial stages of graphene nucleation.

3.3 Following nucleation process starting from the linear carbon chain L6

Now that the formation of linear carbon chains dominates the very first stages of graphene nucleation, it should be a natural deduction that the following nucleation process is very likely to start from the linear carbon chains. Because L6 is a representative linear carbon chain, in this section, some extra carbon atoms have been stepwise imported aside it to simulate the nucleation process starting from a linear chain. The scheme, the adsorption sites used, final optimized configurations obtained and corresponding adsorption energies are illustrated in Fig. 7.

The key point in these simulation results is that it must pass an "energy barrier" of about 0.25 eV (difference of adsorption energy) from the linear chain L6 to the Y-type species L6+1, while, the following nucleation steps to form ring-containing carbon species (L6+2 and L6+3) from L6+1 become almost energetically favored. These results indicate that the formation

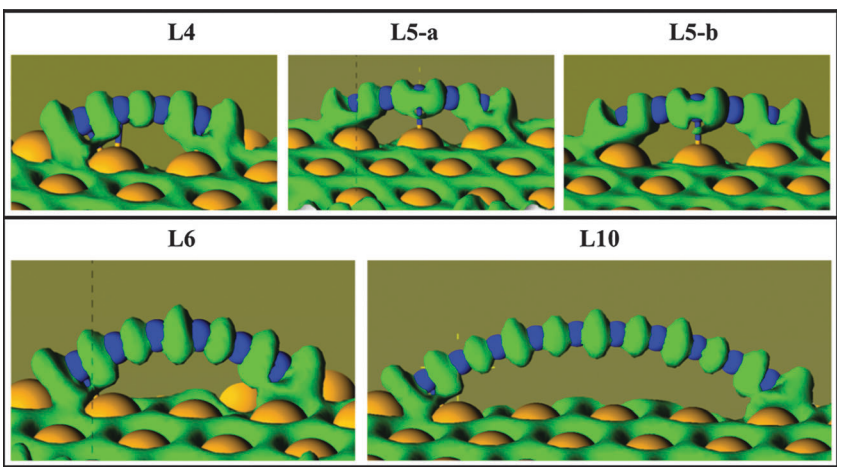

Fig. 6 The deformation electrodensity maps with isovalue 0.01 electrons $Å^{-3}$ in the linear chains. Deformation electrodensity is defined as the total electrodensity with the density of the isolated atoms subtracted.

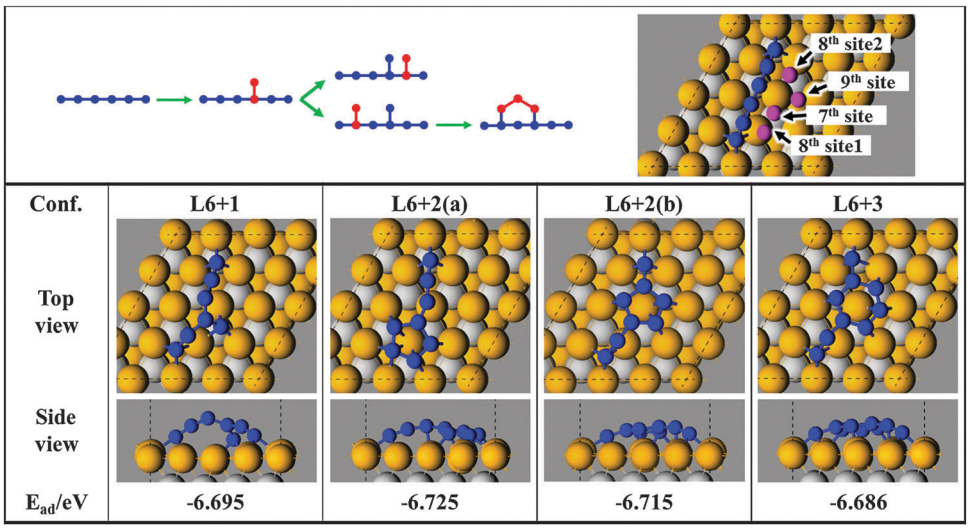

Fig. 7 The scheme, adsorption sites, corresponding optimized configurations and adsorption energies for the attempts to form Y-type and ring-containing structures by importing extra carbon atoms aside a typical linear carbon chain.

of a Y-type structure starting from a linear chain should be the limiting step during the nucleation process of graphene growth on the copper surface.

More broadly, the carbon species Y4, Y5 and Y6-(b–d) (in Fig. 3) could be also regarded as being formed by absorbing an extra carbon aside a 3-, 4- and 5-membered linear chain. In Fig. 5, it could be observed obviously that the adsorption energy in Y4 is about 0.4 eV higher than in C3, in Y5 it is about 0.4 eV higher than in L4, and in Y6 it is about 0.25 eV higher than in L5. That is to say, the formation of a Y-type carbon species based on a longer linear chain is less energetically unfavored. As the energy barrier during the formation of Y6 is quite smaller than that of Y5 and Y4, we infer that the formation of Y-type structures in graphene nucleation is very probable to start from the linear chains having at least five carbon atoms. Another growth path which is not dominant has also been studied and the corresponding results are given in the ESI.†

3.4 An overall nucleation path of graphene growth on the Cu(111) surface

To complete the nucleation process of graphene growth, a 12- and a 18-membered carbon species have been constructed to represent the graphene islands on the Cu(111) surface. For convenience, they are cited as I12 and I18 below. Since what we are concerned about is the law for the absorption energy with an increased carbon number, the most energetically favored structures of carbon clusters having 12 and 18 atoms[35] are not studied. The final configurations of I12 and I18 are given in the ESI,† and the adsorption energies per carbon atom in them are −6.699 and −7.016 eV respectively.

To date, an overall nucleation path of graphene growth on the Cu(111) surface from an isolated carbon atom to a graphene island has been studied completely. Based on the above results we know that, during the nucleation process of graphene, linear chains will be formed firstly, then Y-type carbon species will be formed, and finally ring-containing carbon species till graphene islands will be formed. Here, we pick out the adsorption energies per carbon atom in the carbon species along this nucleation path: C1-a → C2 → C3-a → L4 → L5-a → L6 → L6+1 → L6+2(b) → L6+3 → I12 → I18, and plot them together in Fig. 8.

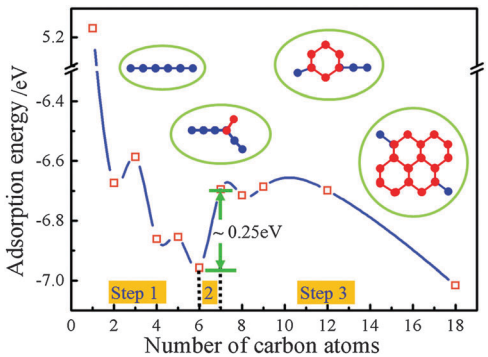

Fig. 8 The energy evolution curve of the overall nucleation path of graphene growth on Cu(111).

Such a nucleation path could be split into three steps. In step 1, linear carbon chains containing 4 to 10 atoms will be formed and dominated the copper surface. In step 2, starting from the linear chains, Y-type carbon species will be shaped when new carbon atoms are absorbed aside them. In step 3, ring-containing carbon species till graphene islands will be formed step-by-step by attaching extra carbon atoms aside the Y-type carbon species gradually.

Step 2 is the nucleation limiting step as it must pass an "energy barrier" of about 0.25 eV. After the Y-type carbon species have been formed, the following formation of ring-containing carbon species and their growth process to form graphene islands should be energetically preferred. The adsorption energy per carbon atom in big enough graphene islands (I18) is even smaller than that in the linear carbon chain L6.

4. Conclusions

The step-by-step atomic nucleation process of graphene growth on a Cu(111) surface is investigated systematically with the aid of DFT calculations. Different from the scheme used in ref. 25, where only one representative two-dimension compact configuration of carbon species with specific size was considered, in this work, a stepwise nucleation process of graphene on the Cu(111) surface by coalescing carbon atoms on an isolated carbon atom is studied by taking all kinds of branched chains and structural motifs in each step. Based on configuration and energy analyses, a three-step overall path of graphene nucleation has been proposed.

At the very first stages of graphene nucleation, the linear chains containing 4 to 10 carbon atoms will be formed and dominate the copper surface, while both the Y-type and circular carbon species are energetically unfavored. Then, based on the formed linear carbon chains, Y-type carbon species will be shaped when some new carbon atoms are absorbed aside them. Finally, with new carbon atoms being attached stepwise, ring-containing carbon species and graphene islands will be formed successively.

The Y-type and ring-containing species are not formed directly at the initial stage of graphene nucleation, but should be formed starting from a linear chain. The 6-membered linear carbon chain should be a representative structure at the initial stages of graphene nucleation, as it is exactly the transition configuration from an on-surface to an arc-shaped linear chain on the copper surface. The nucleation limiting step is the formation of the Y-type carbon species, which must pass an energy barrier of about 0.25 eV. After the Y-type species has been formed, the following nucleation step to form ring-containing carbon species and graphene islands becomes energetically favored.

This investigation provides a comprehensive microscopic picture of the overall atomic path of graphene nucleation on the Cu(111) surface. We hope the underlying observations in this work are instructive to stimulate future experimental efforts on graphene synthesis.

Acknowledgements

This work was partially supported by the National Natural Science Foundation of China (91333122, 51372082, 51172069, 50972032, and 21176132), by the PhD Programs Foundation of Ministry of Education of China (20110036110006 and 20130036110012) and by the Fundamental Research Funds for the Central Universities (Key project 11ZG02, and 12QN16).

References

1 A. K. Geim, *Science*, 2009, **324**, 1530.
2 D. A. C. Brownson, D. K. Kampouris and C. E. Banks, *J. Power Sources*, 2011, **196**, 4873.
3 K. Kim, J.-Y. Choi, T. Kim, S.-H. Cho and H.-J. Chung, *Nature*, 2011, **479**, 338.
4 X. S. Li, W. W. Cai, J. H. An, S. Kim, J. Nah, D. X. Yang, R. Piner, A. Velamakanni, I. Jung, E. Tutuc, S. K. Banerjee, L. Colombo and R. S. Ruoff, *Science*, 2009, **324**, 1312.
5 A. N. Obraztsov, *Nat. Nanotechnol.*, 2009, **4**, 212.
6 S. Bae, H. Kim, Y. Lee, X. F. Xu, J. S. Park, Y. Zheng, J. Balakrishnan, T. Lei, H. R. Kim, Y. I. Song, Y. J. Kim, K. S. Kim, B. Ozyilmaz, J. H. Ahn, B. H. Hong and S. Iijima, *Nat. Nanotechnol.*, 2010, **5**, 574.
7 H. I. Rasool, E. B. Song, M. Mecklenburg, B. C. Regan, K. L. Wang, B. H. Weiller and J. K. Gimzewski, *J. Am. Chem. Soc.*, 2011, **133**, 12536.
8 C. Hwang, K. Yoo, S. J. Kim, E. K. Seo, H. Yu and L. P. Biro, *J. Phys. Chem. C*, 2011, **115**, 22369.
9 X. S. Li, W. W. Cai, L. Colombo and R. S. Ruoff, *Nano Lett.*, 2009, **9**, 4268.
10 K. Celebi, M. T. Cole, K. B. K. Teo and H. G. Park, *Electrochem. Solid-State Lett.*, 2012, **15**, K1.
11 Y. Wu, Y. Hao, H. Y. Jeong, Z. Lee, S. Chen, W. Jiang, Q. Wu, R. D. Piner, J. Kang and R. S. Ruoff, *Adv. Mater.*, 2013, **25**, 6744.
12 H. Kim, C. Mattevi, M. R. Calvo, J. C. Oberg, L. Artiglia, S. Agnoli, C. F. Hirjibehedin, M. Chhowalla and E. Saiz, *ACS Nano*, 2012, **6**, 3614.
13 L. Meng, Q. Sun, J. Wang and F. Ding, *J. Phys. Chem. C*, 2012, **116**, 6097.
14 H. Amara, C. Bichara and F. Ducastelle, *Phys. Rev. B: Condens. Matter Mater. Phys.*, 2006, **73**, 113404.
15 H. Amara, C. Bichara and F. Ducastelle, *Phys. Rev. Lett.*, 2008, **100**, 056105.
16 H. Amara, J. M. Roussel, C. Bichara, J. P. Gaspard and F. Ducastelle, *Phys. Rev. B: Condens. Matter Mater. Phys.*, 2009, **79**, 014109.
17 X. Mi, V. Meunier, N. Koratkar and Y. Shi, *Phys. Rev. B: Condens. Matter Mater. Phys.*, 2012, **85**, 155436.
18 S. Saadi, F. Abild-Pedersen, S. Helveg, J. Sehested, B. Hinnemann, C. C. Appel and J. K. Nørskov, *J. Phys. Chem. C*, 2010, **114**, 11221.
19 Y. Li, M. Li, T. Gu, F. Bai, Y. Yu, T. Mwenya and Y. Yu, *AIP Adv.*, 2013, **3**, 052130.
20 Z. T. Luo, S. Kim, N. Kawamoto, A. M. Rappe and A. T. C. Johnson, *ACS Nano*, 2011, **5**, 9154.
21 H. Chen, W. G. Zhu and Z. Y. Zhang, *Phys. Rev. Lett.*, 2010, **104**, 186101.
22 P. Wu, W. H. Zhang, Z. Y. Li, J. L. Yang and J. G. Hou, *J. Chem. Phys.*, 2010, **133**, 071101.
23 S. Riikonen, A. Krasheninnikov, L. Halonen and R. Nieminen, *J. Phys. Chem. C*, 2012, **116**, 5802.
24 Y. Li, M. Li, T. Gu, F. Bai, Y. Yu, M. Trevor and Y. Yu, *Appl. Surf. Sci.*, 2013, **284**, 207.
25 R. G. Van Wesep, H. Chen, W. Zhu and Z. Zhang, *J. Chem. Phys.*, 2011, **134**, 171105.
26 J. Gao and J. Zhao, *Eur. Phys. J. D*, 2013, **67**, 1.
27 P. Wu, H. Jiang, W. Zhang, Z. Li, Z. Hou and J. Yang, *J. Am. Chem. Soc.*, 2012, **134**, 6045.
28 J. Gao, J. Yip, J. Zhao, B. I. Yakobson and F. Ding, *J. Am. Chem. Soc.*, 2011, **133**, 5009.

29 O. V. Yazyev and A. Pasquarello, *Phys. Rev. Lett.*, 2008, **100**, 156102.
30 B. Delley, *J. Chem. Phys.*, 1990, **92**, 508.
31 B. Delley, *J. Chem. Phys.*, 2000, **113**, 7756.
32 J. P. Perdew, K. Burke and M. Ernzerhof, *Phys. Rev. Lett.*, 1996, **77**, 3865.
33 D. Cheng, G. Barcaro, J. C. Charlier, M. Hou and A. Fortunelli, *J. Phys. Chem. C*, 2011, **115**, 10537.
34 J. Gao, Q. Yuan, H. Hu, J. Zhao and F. Ding, *J. Phys. Chem. C*, 2011, **115**, 17695.
35 Q. Yuan, J. Gao, H. Shu, J. Zhao, X. Chen and F. Ding, *J. Am. Chem. Soc.*, 2011, **134**, 2970.